Journal of Applied Statistics

ISSN: (Print) (Online) Journal homepage: https://www.tandfonline.com/loi/cjas20

Capturing spatiotemporal dynamics of Alaskan groundfish catch using signed-rank estimation for varying coefficient models

H. E. Correia & A. Abebe

To cite this article: H. E. Correia & A. Abebe (2021): Capturing spatiotemporal dynamics of Alaskan groundfish catch using signed-rank estimation for varying coefficient models, Journal of Applied Statistics, DOI: 10.1080/02664763.2021.1889996

To link to this article: https://doi.org/10.1080/02664763.2021.1889996

JOURNAL OF APPLIED STATISTICS
https://doi.org/10.1080/02664763.2021.1889996

Taylor & Francis
Taylor & Francis Group

Capturing spatiotemporal dynamics of Alaskan groundfish catch using signed-rank estimation for varying coefficient models

H. E. Correia [a,b,c] and A. Abebe [a]

[a]Department of Mathematics and Statistics, Auburn University, Auburn, AL, USA; [b]Harvard Data Science Initiative, Harvard University, Cambridge, MA , USA; [c]Department of Biostatistics, Harvard University, Boston, MA, USA

ABSTRACT

Varying coefficient models (VCMs) are commonly used for their high degree of flexibility in modeling complex systems. Many applications in fisheries utilize VCMs to capture spatial variation in populations of marine fishes. All of these applications use the penalized least squares method for estimation. However, this approach is known to be sensitive to non-normal distributions and outliers, a common feature of ecological data. Robust estimation methods are more appropriate for handling noisy and non-normal data. We present the application of a signed-rank-based procedure for obtaining robust estimates in VCMs on a fisheries dataset from the North Pacific Ocean. We demonstrates that the signed-rank-based estimation method provides better fit and improved prediction in comparison to the classical likelihood VCM fits in both simulations and the real data application, particularly when the distributions are non-normal and may be misspecified. Rank-based estimation of VCMs is therefore valuable for modeling ecological data and obtaining useful inferences where non-normality and outliers are common.

ARTICLE HISTORY
Received 2 June 2020
Accepted 9 February 2021

KEYWORDS
Robust estimation; signed-rank; varying coefficient models; Alaska groundfish

1. Introduction

The modeling of species distributions, a significant endeavor in ecology and conservation, has become a more prominent feature of population analyses as improvements in technology and cost efficiency have increased the ability to collect spatial ecological data. Statistical research has greatly developed the theory of models containing spatial autocorrelation during the past half century [52], however the application of these methods has only recently been considered valuable to modeling ecological processes [12,23,29,30]. A popular statistical method for modeling species distributions and abundance is the varying coefficient model (VCM) [6,19] introduced by Hastie and Tibshirani [21]. While the importance of

CONTACT H. E. Correia hcorreia@hsph.harvard.edu Department of Mathematics and Statistics, Auburn University, Auburn, AL 36849, USA; Harvard Data Science Initiative, Harvard University, Cambridge, MA 02138, USA; Department of Biostatistics, Harvard University, Boston, MA 02115, USA

Supplemental data for this article can be accessed here. https://doi.org/10.1080/02664763.2021.1889996

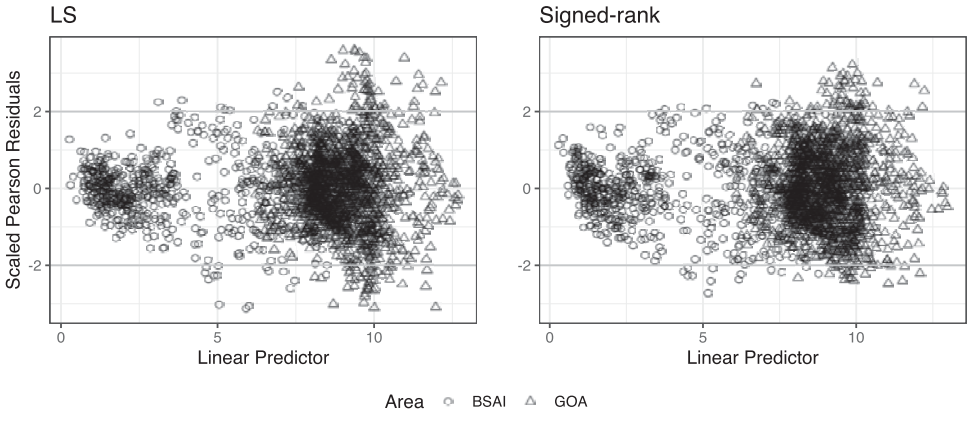

Figure 1. Scaled Pearson residuals plotted by area for sablefish CPUE modeled with a spatiotemporally variant sea surface temperature fit using penalized least squares (LS) or the signed-rank procedure. BSAI = Bering Sea and Aleutian Islands; GOA = Gulf of Alaska.

modeling spatial variation in marine systems is a relatively new focus, VCMs are becoming popular for modeling spatial and spatiotemporal marine data due to the flexibility of including georeferenced data using appropriate smoothers to model spatial dependence [54]. With the identification of regime shifts in several large marine ecosystems [15,47], the modeling of spatiotemporal variation in marine systems is becoming crucial to manage vulnerable populations in response to climate change.

Ecological and climate data often exhibit outliers that may be informative to the analyses. Outliers in spatial data contribute to trends over space that factor into understanding the system, therefore removing outliers or transforming the data are not suitable alternatives. The fisheries dataset analyzed in this paper is a strong illustration of this issue. We fit a spatiotemporal model using the classical least squares (LS) fitting and our proposed signed-rank-based approach for sablefish catches in the Gulf of Alaska (GOA) and Bering Sea/Aleutian Islands (BSAI) with sea surface temperature (SST) as a spatiotemporally varying covariate. Figure 1 gives the scaled residual plots of these fits with the signed-rank-based approach. It can be seen that outliers occur with higher incidence in some of the locations in the North Pacific when modeling sablefish catch in this formulation. The influence of outliers on the model is far greater for the classical VCM estimation in comparison to the signed-rank-based approach. While such large deviations are common in fisheries data, they have not been explicitly addressed, and the issue becomes a concern when using VCMs to fit these types of data. The application of our signed-rank-based approach to this fisheries data will be discussed in detail at the end of this paper.

Section 2 gives the VCM and a brief description of the signed-rank-based methodology as applied to VCMs. Section 3 provides simulations that test the performance of the signed-rank estimator of VCMs against least squares and least absolute deviations estimators in an intercept-only model and a more complex model under a variety of settings. Section 4 revisits our motivating question from fisheries data and provides a more detailed analysis with three-dimensional covariates.

2. Methodology

The VCM introduced in [10] extends the linear regression model to one where the regression coefficients may depend on certain covariates. Given a response variable Y and covariate vectors $\mathbf{u} = (u_1, \ldots, u_q)^\top$ and $\mathbf{x} = (x_1, \ldots x_p)^\top$, the VCM is defined by

$$Y = g_0(\mathbf{u}) + g_1(\mathbf{u})x_1 + \cdots + g_p(\mathbf{u})x_p + \varepsilon \,, \tag{1}$$

where the functions $g_k : \mathbb{R}^q \to \mathbb{R}$, $k = 0, \ldots, p$ are all assumed to be smooth functions. The random error ε is assumed to have a probability density function f with finite Fisher information; that is, $\int (f')^2/f < \infty$.

The VCM is often used in the context of the analysis of longitudinal data where $\mathbf{u}$ will be a univariate time variable. This is known as a time-varying coefficient model (e.g. [9]). When $\mathbf{u}$ represents a spatial location, then the models are known as spatially-varying coefficient models [17]. The flexibility of these models has made them attractive for use in geostatistics [20] and medical imaging [56]. Our application will use a spatiotemporally-varying coefficient model for marine populations. Such models have been studied and applied in the past (e.g. [32]).

Signed-rank-based estimation depends on minimization of the weighted L_1 norm defined as

$$\|\mathbf{x}\|_{\varphi^+} = \sum_{i=1}^{n} \varphi^+ \left(\frac{R(|x_i|)}{n+1} \right) |x_i| \,, \quad \mathbf{x} \in \mathbb{R}^n \,,$$

where $R(x_i)$ is the rank of x_i among $x_1, \ldots, x_n$ and $\varphi^+ : (0,1) \to \mathbb{R}^+$ is a non-decreasing, square-integrable function [22]. The Wilcoxon estimator is found by taking $\varphi^+(u) = u$ and the least absolute deviations (LAD) estimator is found by taking $\varphi^+(u) = 1$. Unless explicitly stated, we will refer to the Wilcoxon estimator as the generic signed-rank (SR) estimator.

We are interested in the SR estimator of the VCM given in (1). Given n sample data points $\{\mathbf{u}_j, \mathbf{x}_j, Y_j\}$, where $\mathbf{u} \in \mathbb{R}^q, \mathbf{x} \in \mathbb{R}^p, Y \in \mathbb{R}$ for $j = 1, 2, \ldots, n$, the VCM is written as

$$Y_j = g_0(\mathbf{u}_j) + g_1(\mathbf{u}_j)x_{1j} + \cdots + g_p(\mathbf{u}_j)x_{pj} + \varepsilon_j \,, \tag{2}$$

where the unobserved random errors $\varepsilon_j|_{j=1}^n$ are assumed to be independent and identically distributed following a symmetric distribution with median 0.

To define the SR estimator of the VCM coefficient functions, we will follow the local linear approximation approach of Fan and Gijbels [14]. The VCM errors can be written as

$$\varepsilon_j = Y_j - \sum_{k=0}^{p} g_k(\mathbf{u}_j)x_{kj} \,, \mathbf{x}_0 = 1 \qquad j = 1, 2, \ldots, n \,.$$

Since the coefficient functions g_k are smooth, they can be approximated by a tensor-product smooth

$$g_k(\mathbf{u}_j) \approx \sum_{i_1=1}^{L_1} \cdots \sum_{i_q=1}^{L_q} \gamma_{k,i_1,\ldots,i_q} \mathscr{B}_{k,i_1}(u_{j1}) \cdots \mathscr{B}_{k,i_q}(u_{jq}) \,, \quad k = 0, \ldots, p \,; j = 1, \ldots, n \,,$$

where $\mathscr{B}_k(\cdot)$ are the B-spline basis functions with a fixed degree and knot sequence. The spline coefficients can be written as a $(L_1 \times \cdots \times L_q)$-vector $\boldsymbol{\gamma}_k$ and $g_k(\mathbf{u}_j)$ can be written

as

$$g_k(\mathbf{u}_j) = \boldsymbol{\gamma}_k^\top \mathbf{Z}_k(\mathbf{u}_j)$$

where

$$\mathbf{Z}_k(\mathbf{u}_j) = \bigotimes_{i=1}^{q} \mathbf{b}_{ki}(u_{ji})$$

where $\bigotimes$ is the Kronecker product and $\mathbf{b}_{ki}(u_{ji}) = (\mathscr{B}_{k,i}(u_{ji}), \ldots, \mathscr{B}_{k,L_i}(u_{ji}))^\top$. Model (2) can now be approximated by

$$Y_j \approx \sum_{k=0}^{p} \{\mathbf{Z}_k(\mathbf{u}_j)^\top \boldsymbol{\gamma}_k\} x_{kj} + \varepsilon_j \quad .$$

Now, define the residuals as $r_j(\boldsymbol{\Gamma}) = Y_j - \sum_{k=0}^{p} \{\mathbf{Z}_k(\mathbf{u}_j)^\top \boldsymbol{\gamma}_k\} x_{kj}$, where $\boldsymbol{\Gamma} = (\boldsymbol{\gamma}_0^\top, \ldots, \boldsymbol{\gamma}_p^\top)^\top$. The signed-rank objective function given in [33] is now defined by

$$Q_n(\boldsymbol{\Gamma}) = \frac{1}{n} \sum_{i=1}^{n} \varphi^+ \left(\frac{R(|r_j(\boldsymbol{\Gamma})|)}{n+1} \right) |r_j(\boldsymbol{\Gamma})| \, .$$

The procedure for obtaining the SR estimates $\widehat{g}_k$ proceeds using the iteratively re-weighted least squares algorithm of [42] as follows:

Step 1: Let $\epsilon_w > 0$ be a given tolerance. For $j = 1, \ldots, n$, define

$$w_j(\boldsymbol{\Gamma}) = \begin{cases} \dfrac{\varphi^+ \left(\dfrac{R(|r_j(\boldsymbol{\Gamma})|)}{n+1} \right)}{|r_j(\boldsymbol{\Gamma})|} & \text{if } |r_j(\boldsymbol{\Gamma})| > \epsilon_w \\ 0 & \text{if } |r_j(\boldsymbol{\Gamma})| \leq \epsilon_w \end{cases}$$

Step 2: Given an initial estimate $\widehat{\boldsymbol{\Gamma}}^{(0)}$, minimize

$$Q(\boldsymbol{\Gamma} | \widehat{\boldsymbol{\Gamma}}^{(0)}) = \sum_{j=1}^{n} w_j \left(\widehat{\boldsymbol{\Gamma}}^{(0)} \right) r_j^2(\boldsymbol{\Gamma})$$

resulting in $\widehat{\boldsymbol{\Gamma}}^{(1)}$. This can be performed using the weighted GAM implemented in the ***mgcv*** package [53] of R [39].

Step 3: Check if

$$\frac{\| \widehat{\boldsymbol{\Gamma}}^{(1)} - \widehat{\boldsymbol{\Gamma}}^{(0)} \|_*}{\| \widehat{\boldsymbol{\Gamma}}^{(0)} \|_*} < \epsilon \, ,$$

where $\| \cdot \|_*$ is the Frobenius matrix norm. If true, **STOP**. If false, take $\widehat{\boldsymbol{\Gamma}}^{(0)} \leftarrow \widehat{\boldsymbol{\Gamma}}^{(1)}$ and go back to **Step 2**.

As noted in the algorithm, the iterative procedure can be executed simply within the R environment as a modification to the ***mgcv*** package. Code to obtain SR estimates in this manner is provided in the supplementary material.

3. Simulations

The following simulations reflect how the signed-rank (SR) estimator of VCMs performs against least squares (LS) and least absolute deviation (LAD) estimators in a variety of settings for finite samples.

3.1. Intercept model with 2D coefficient function

We considered the simple intercept model

$$Y_j = g_0(\mathbf{u}_j) + \varepsilon_j\,, \quad j = 1, \ldots, n\,,$$

where $\mathbf{u}_j = (x_j, z_j)'$ and g_0 is given by

$$g_0(\mathbf{u}_j) = (\pi^{s_x} s_z)(1.2)\exp\left(-\frac{(x_j - 0.2)^2}{s_x^2} - \frac{(z_j - 0.3)^2}{s_z^2}\right) + (0.8)\exp\left(-\frac{(x_j - 0.7)^2}{s_x^2} - \frac{(z_j - 0.8)^2}{s_z^2}\right)$$

with $s_x = 0.3$, $s_z = 0.4$, and x and z are 100 random deviates generated from a continuous uniform distribution with range $[0, 1]$. The correlation between two observations a distance r apart was $\exp(-(r/d)^2)$. The relative efficiencies of the SR and LAD estimators versus the LS estimator were obtained as

$$\mathrm{RE(SR, LS)} = \frac{\sum_{j=1}^{n}(g_0(\mathbf{u}_j) - \hat{g}_{\mathrm{LS}}(\mathbf{u}_j))^2}{\sum_{j=1}^{n}(g_0(\mathbf{u}_j) - \hat{g}_{\mathrm{SR}}(\mathbf{u}_j))^2} \quad \text{and}$$

$$\mathrm{RE(LAD, LS)} = \frac{\sum_{j=1}^{n}(g_0(\mathbf{u}_j) - \hat{g}_{\mathrm{LS}}(\mathbf{u}_j))^2}{\sum_{j=1}^{n}(g_0(\mathbf{u}_j) - \hat{g}_{\mathrm{LAD}}(\mathbf{u}_j))^2}\,,$$

respectively. Here with $\hat{g}_{\mathrm{LS}}$, the function g was estimated using the classical least squares (LS) approach. Similarly, $\hat{g}_{\mathrm{SR}}$ and $\hat{g}_{\mathrm{LAD}}$ represent the fitted values using the SR and LAD methods, respectively. The R^2 values of the LS, SR, and LAD fits were calculated as functions of the correlations $R^2 = \rho^2(g, \hat{g}_a)$ with $\hat{g}_a$, $a = \mathrm{LS, SR, LAD}$, being the model predictions and g being the true function. We use R^2 not as a measure of variance explained but rather to compare fits among various estimation methods. We obtain both the LAD and SR estimators using the penalized weighted LS approach with the LS estimator as the initial value, where we use the score function $\varphi^+(u) = 1$ for LAD and the Wilcoxon score function $\varphi^+(u) = \sqrt{3}u$ for SR estimators in the weight function. These are scaled so that $\int_0^1(\varphi^+(u))^2\mathrm{d}u = 1$ which simplifies the form of the asymptotic variance expression. Out-of-sample prediction performance was assessed by using the fitted model to produce predictions given new test data of $m = 25$ samples. The mean squared prediction errors (MSPE) for methods $a = \mathrm{LS, SR, LAD}$ were obtained as

$$\mathrm{MSPE}_a = \frac{1}{m}\sum_{i=1}^{m}(g_0(\mathbf{u}_i) - \hat{g}_a(\mathbf{u}_i))^2\,.$$

The following simulations were performed on $n = 100$ samples and repeated for 1000 iterations.

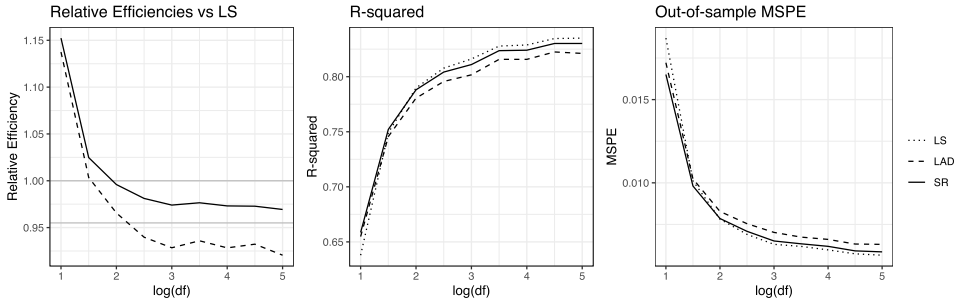

Figure 2. Heavy-tailed distribution relative efficiencies, R^2 values, and out-of-sample mean squared prediction errors (MSPE) for increasing $\log(df)$. Horizontal lines at $3/\pi$ and 1 indicate relative efficiency values for the Wilcoxon and LS procedures, respectively.

The first simulation involved testing the performance of VCM estimators in the presence of heavy-tailed error distributions. To simulate this, the errors ε_j were randomly generated from Student's t distributions with increasing degrees of freedom e^k, where k is taken from 1 to 5 in steps of 0.5. The correlation between two observations a distance r apart was $\exp(-(r/d)^2)$ with $d = 0.1$. VCMs were fit for the given data using LS, LAD, and SR methods. The relative efficiencies and R^2 values were then calculated as described above and plotted for logarithms of the corresponding degrees of freedom, $k = \log(df)$ (Figure 2).

The left panel of Figure 2 shows that both LAD and SR estimators are more efficient than the LS estimator when the error distribution is heavy-tailed. As expected, the efficiency drops as the tails of the generated distribution approach the tails of the normal distribution. However, the loss in efficiency is less than 5% for the SR method. This is in line with the theoretical asymptotic relative efficiency value of $3/\pi$ for the Wilcoxon procedure. The LAD estimator is generally less efficient than the SR estimator. The center panel of Figure 2 shows that all methods provide improved fit as the tails of the error distribution approach $N(0, 1)$ tails, with the SR procedure giving slightly better fit for heavy tails and LS giving slightly better fit for tails approaching $N(0, 1)$. Similarly, the right panel reveals that the SR procedure produced the lowest out-of-sample prediction errors for heavy tails, while LS gave the lowest prediction errors for tails approaching $N(0, 1)$.

The second simulation tested VCM estimation performance when there are outliers in the measured response. To simulate this, we generated random errors ε_j drawn from a contaminated normal distribution. The contaminated normal distribution is defined by creating a normal-normal Huber contaminated distribution as

$$CN(\tau, \sigma) = (1 - \tau)N(0, 1) + \tau N(0, \sigma^2) \,,$$

where $\tau \in [0, 1]$ and $\sigma > 0$. This means the errors are drawn from the $N(0, 1)$ distribution with probability $1 - \tau$ and from the $N(0, \sigma^2)$ distribution with probability τ. For our simulation experiment, we took $\sigma = 3$ and τ taken from 0 to 0.15 in steps of 0.05. Once again, the correlation between two observations a distance r apart is $\exp(-(r/d)^2)$ with $d = 0.1$. Relative efficiencies versus LS and R^2 values were plotted against the proportion of contamination in Figure 3. The left panel shows that both LAD and SR estimators were more efficient than LS estimators for greater than 5% contamination. The center panel of

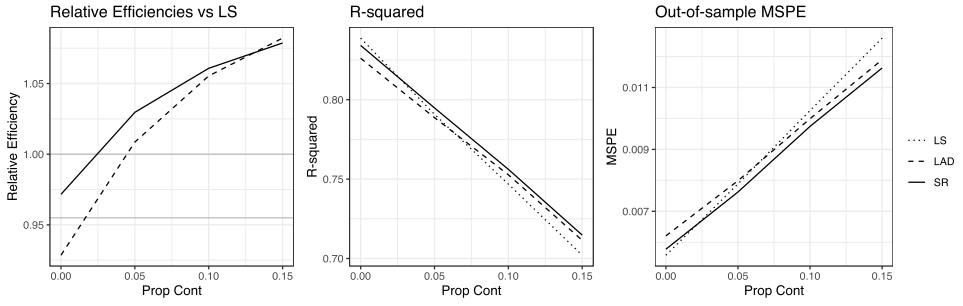

Figure 3. Relative efficiencies, R^2 values, and out-of-sample mean squared prediction errors (MSPE) for increasing proportions of contamination of the normal distribution. Horizontal lines at $3/\pi$ and 1 indicate relative efficiency values for the Wilcoxon and LS procedures, respectively.

Figure 3 shows that the SR method produced marginally better fitting models for contamination greater than 5%, while the right panel shows that the SR method also produced the smallest out-of-sample prediction errors for greater than 5% contamination.

The performance of VCM estimators under various levels of spatial clustering was analyzed in the third simulation. The errors ε_j were drawn from a normal distribution centered at zero with standard deviation of one. The correlation between two observations a distance r apart was $\exp(-(r/d)^2)$ with d taken from 0.1 to 0.35 in steps of 0.05 for varying correlation structure. These represent weak clustering (almost independence) to strong clustering of the spatial data. Relative efficiencies versus LS and R^2 were calculated as before. These were plotted against increasing correlation between observations (Figure 4).

The left panel of Figure 4 shows that the SR estimator was more efficient than LAD and both are less efficient than LS when the errors have low spatial correlation. However, the loss in efficiency for the SR procedure in comparison to LS ranged from 3% for low spatial correlation to 0% for high spatial correlation. The center panel of Figure 3 shows that the SR procedure produced marginally poorer fitting models than LS for low spatial correlation and virtually the same fit when the spatial correlation was large. Additionally,

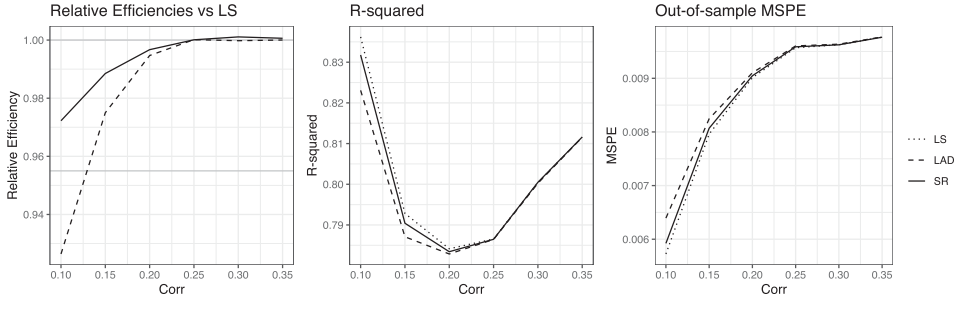

Figure 4. Relative efficiencies, R^2 values, and out-of-sample mean squared prediction errors (MSPE) for increasing spatial correlations in data. Horizontal lines at $3/\pi$ and 1 indicate relative efficiency values for the Wilcoxon and LS procedures, respectively.

the right panel of Figure 3 shows that the LS procedure had marginally smaller out-of-sample prediction errors than SR for low spatial correlation, and the SR procedure had nearly identical prediction error values to LS and LAD for high spatial correlation. We note that all methods gave poorer fits as the correlation increased from $d = 0.10$ to $d = 0.20$, but the fits appear to improve when correlation was increased further. The appearance of improved fits for larger spatial autocorrelation is likely due to overfitting [54].

3.2. A 4-variable model

We then considered the model

$$Y_j = g_0(u_j) + g_1(u_j)x_1 + g_2(u_j)x_2 + g_3(u_j)x_3 + g_4(u_j)x_4 + \varepsilon_j\,, \quad j = 1, \ldots, n\,,$$

where $g_0(u_j) = 1 + 3u_j^2, g_1(u_j) = 3\exp(-u_j^2), g_2(u_j) = 1.5\sin(\pi u_j), g_3(u_j) = 0.8u_j, g_4(u_j) = 0$, $\mathbf{x}_j = (x_1, x_2, x_3, x_4)'$ was generated from the multivariate normal distribution with mean 0 and $Cov(x_k, x_m) = 0.5^{|k-m|}$, and u_j was generated from the Uniform$(-1, 1)$ distribution. The zero function $g_4(u_j)$ was used to explore whether the SR method could estimate an unnecessary term in the model adequately. Errors ε_j were generated from one of three distributions considered: a standard normal distribution, $N(0, 1)$; a contaminated normal distribution, $CN(0.95)$, with contamination rate of 0.05; or a Student's t distribution with 3 degrees of freedom, $t(3)$. Simulations were performed on $n = 200$ and $n = 400$ samples and repeated for 500 iterations. The functions g_k were estimated using the penalized LS method and the SR method. For each smooth, the mean squared error (MSE) across all $T = 500$ iterations for each estimation method was calculated as

$$\text{MSE}(g_k) = \frac{1}{T}\sum_{p=1}^{T}\left(\sum_{i=1}^{n}\frac{(g_k - \hat{g}_k)^2}{n}\right)\,.$$

For visual comparison, the estimated smooth functions from each method for each g_k were also plotted for the 500 iterations with the true functions overlaid. We constructed a test data set of $m = 50$ for the $n = 200$ sample set and $m = 100$ for the $n = 400$ sample set to compare the out-of-sample prediction performance of the proposed method to the LS method. The mean squared prediction error (MSPE) across all $T = 500$ iterations was calculated for each smooth for the SR and LS methods as

$$\text{MSPE}(g_k) = \frac{1}{T}\sum_{p=1}^{T}\left(\sum_{i=1}^{m}\frac{(g_k - \hat{g}_k)^2}{m}\right)\,.$$

For the model with errors drawn from $N(0, 1)$, the SR method was on par with LS, with MSE approximately equal between both methods for all estimated coefficient functions even as sample size increased (Figure 5). This was similarly observed for predictions made on test data (Figure 6). SR estimation of the model with errors drawn from $CN(0.95)$ was more accurate than the LS method, particularly at the boundaries of the functions (Figure 7). The same was true for the model with errors generated from the $t(3)$ distribution (Figure 9). Out-of-sample predictions from the SR method were also more accurate than LS for the $CN(0.95)$ and $t(3)$ errors (Figures 8 and 10). MSE and MSPE were consistently lower for coefficient functions estimated for training data and predicted for test

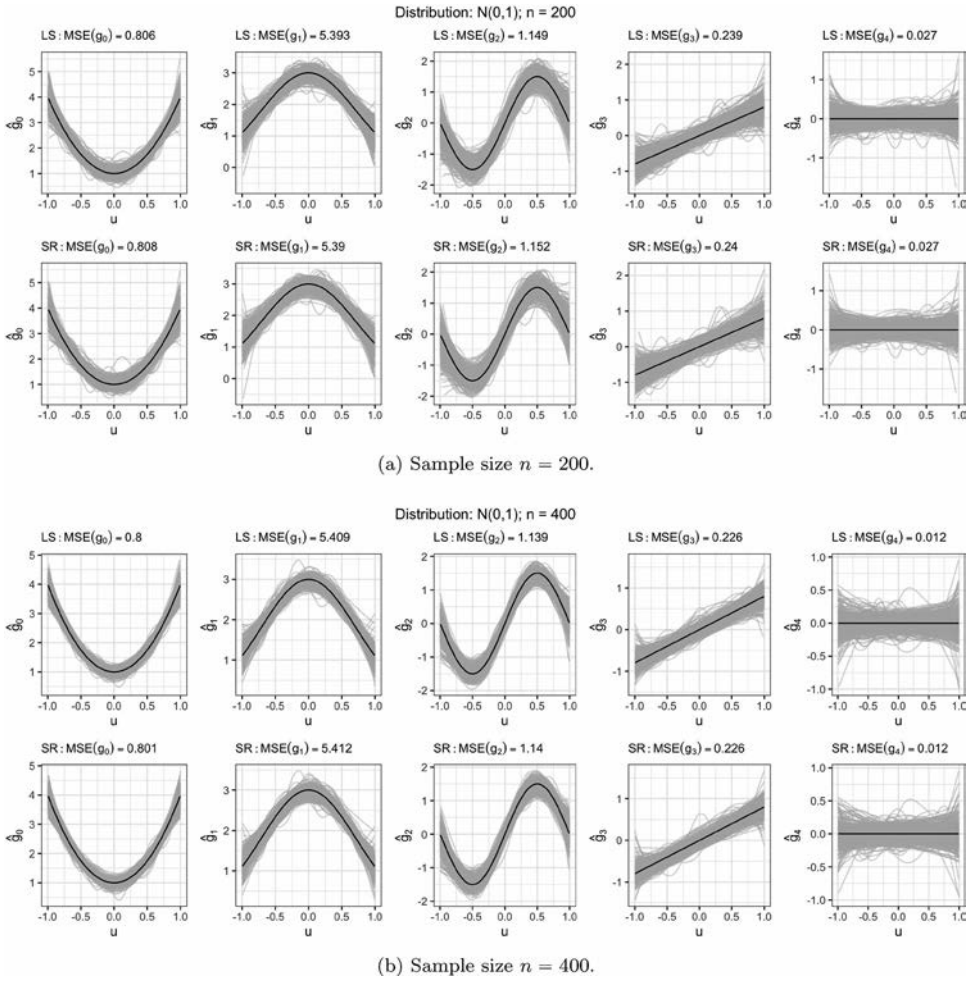

Figure 5. Individual smooths $\{g_0, g_1, g_2, g_3, g_4\}$ for a varying coefficient model with $N(0, 1)$ errors estimated using penalized least squares (LS) and signed-rank (SR) methods for 500 simulations (in grey), with the true functions overlaid in black.

data using the SR method for models with errors from $CN(0.95)$ and $t(3)$. As expected, the SR method outperformed the LS method for contaminated and heavy-tailed distributions, and the SR method was more accurate in its estimation and prediction of the zero function for these types of distributions.

4. Application

In this section, we compare SR-based VCM fitting with the penalized LS approach in modeling catches of sablefish (*Anoplopoma fimbria*) and Pacific cod (*Gadus macrocephalus*) in the Gulf of Alaska. The data for this study were obtained from the National Oceanic and Atmospheric Administration (NOAA) for download to the public. The annual longline survey of the Marine Ecology and Stock Assessment (MESA) Program drops baited lines

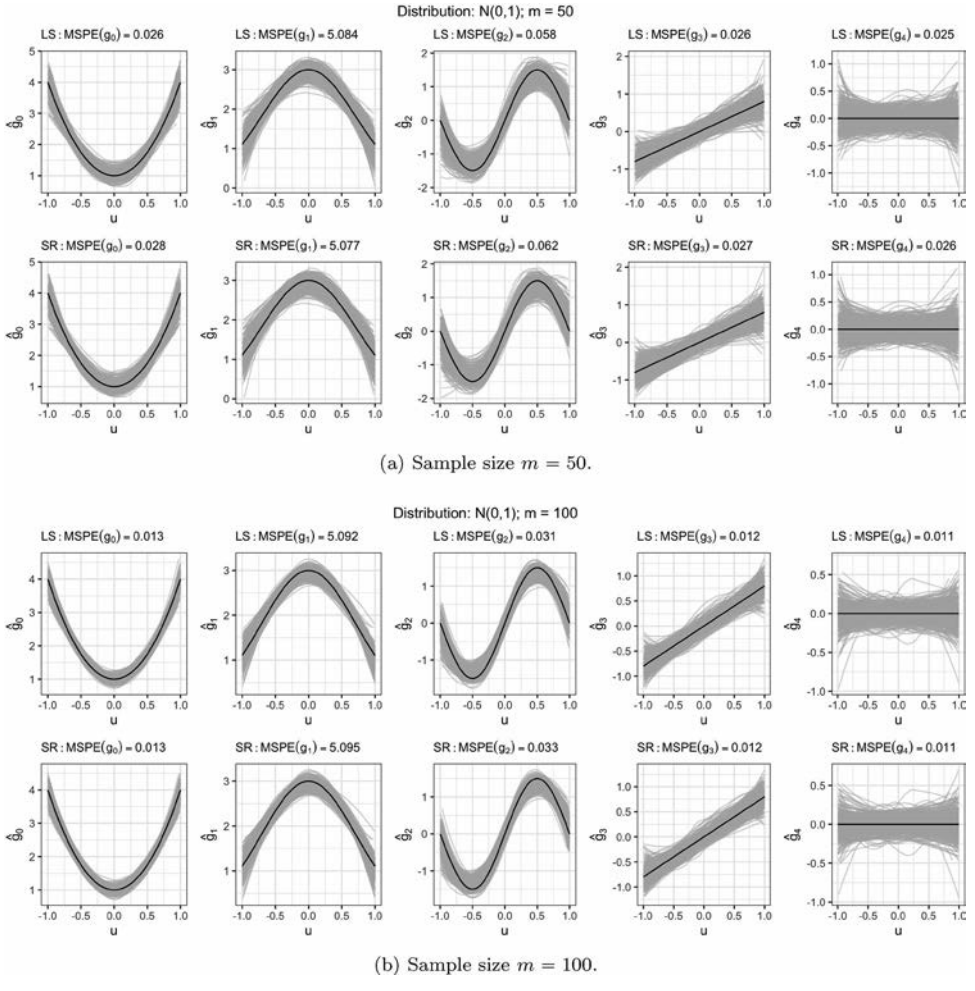

Figure 6. Individual smooths $\{g_0, g_1, g_2, g_3, g_4\}$ for a varying coefficient model with $N(0, 1)$ errors predicted for a test data set of size m using penalized least squares (LS) and signed-rank (SR) methods for 500 simulations (in grey), with the true functions overlaid in black.

at specific locations ('stations') off the coast of Alaska to catch groundfish species along the entire coast [1]. A catch per unit effort (CPUE) is calculated for each species within each geographic area [13]. MESA data were acquired for the years of 1979 through 2012. Sea surface temperature (SST) measured every three to six hours for corresponding locations and years 1982 through 2012 were obtained from infrared satellite sensors via the National Centers for Environmental Information [35]. SST is considered an important factor for recruitment in many fish species: since sablefish and cod larvae inhabit shallow coastal zones, they are likely to be directly affected by fluctuations in SST. Juvenile sablefish are believed to be particularly sensitive to water temperature changes [43,44], and Pacific cod show similar sensitivities, especially in growth rates and survival [25,27,28]. Since sablefish and Pacific cod spawn in deep waters in late winter and early spring, seasonal amplitude of SST was calculated as the mean of June, July, and August minus the mean of December,

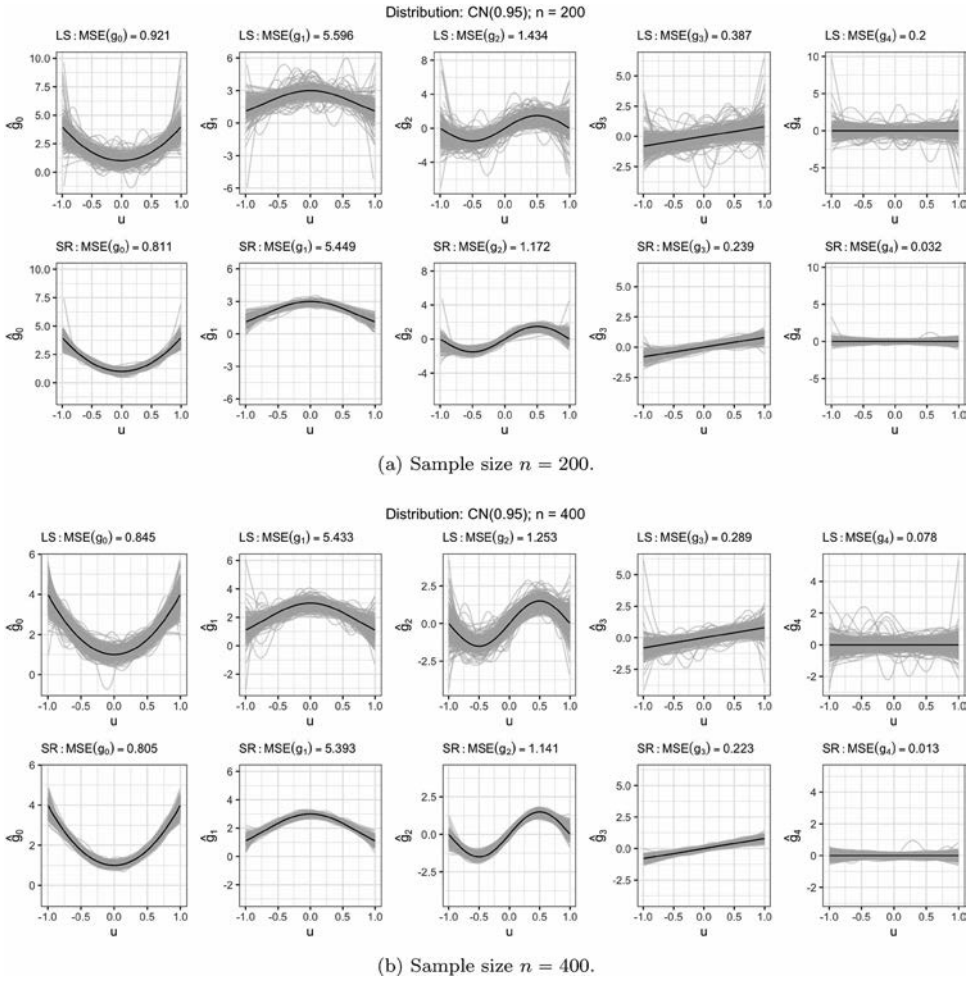

Figure 7. Individual smooths $\{g_0, g_1, g_2, g_3, g_4\}$ for a varying coefficient model with $CN(0.95)$ errors estimated using penalized least squares (LS) and signed-rank (SR) methods for 500 simulations (in grey), with the true functions overlaid in black.

January, and February. In addition, sablefish and Pacific cod are not substantially recruited to longline gear in their adult habitat until at least five years of age [2,7,37], therefore SST measures were lagged by five years to consider the effect of temperature on the juvenile stage of the population entering recruitment.

In this example, we focused on determining the spatial catch densities of Pacific cod and sablefish and whether inclusion of spatiotemporally varying SST improved model prediction, a key goal for managers. Two models were fit for each species' CPUE and included three main factors expected to affect population dynamics: location in the form of latitude-longitude pairs, time in the form of years, and environment in the form of seasonal amplitude of SST lagged by five years.

The intercept model considered was

$$Y_{(u,v,t)} = z_1(u, v, t) + \varepsilon_{(u,v,t)} \,, \tag{3}$$

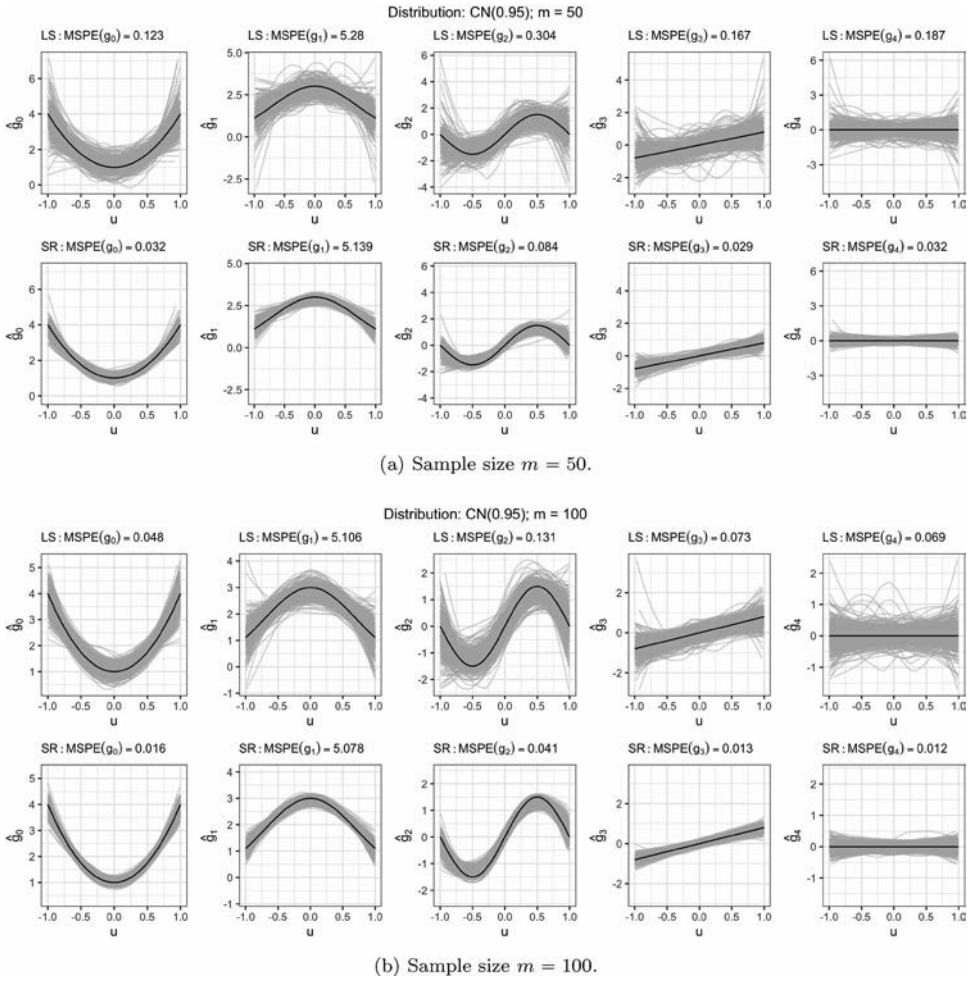

Figure 8. Individual smooths $\{g_0, g_1, g_2, g_3, g_4\}$ for a varying coefficient model with $CN(0.95)$ errors predicted for a test data set of size m using penalized least squares (LS) and signed-rank (SR) methods for 500 simulations (in grey), with the true functions overlaid in black.

where t is time in years from 1982 to 2012, u is latitude, v is longitude, and z_1 is a three-dimensional tensor smoothing function. There were a total of 2877 observations for sablefish and 2297 observations for Pacific cod. The sablefish CPUE was roughly symmetric. However, Pacific cod CPUE values were right skewed and were therefore modeled via two separate approaches: a symmetric distribution assumption where SR estimation was fit using the Wilcoxon score function and a right-skewed distribution assumption where a bent score function [26] was used to accommodate skewness in the response distribution. The bent scores were generated using the score function

$$\varphi^{+}(u) = \begin{cases} \dfrac{4\sqrt{2}}{3}u\,, & u < 3/4 \\ \sqrt{2}\,, & u \geq 3/4\,. \end{cases}$$

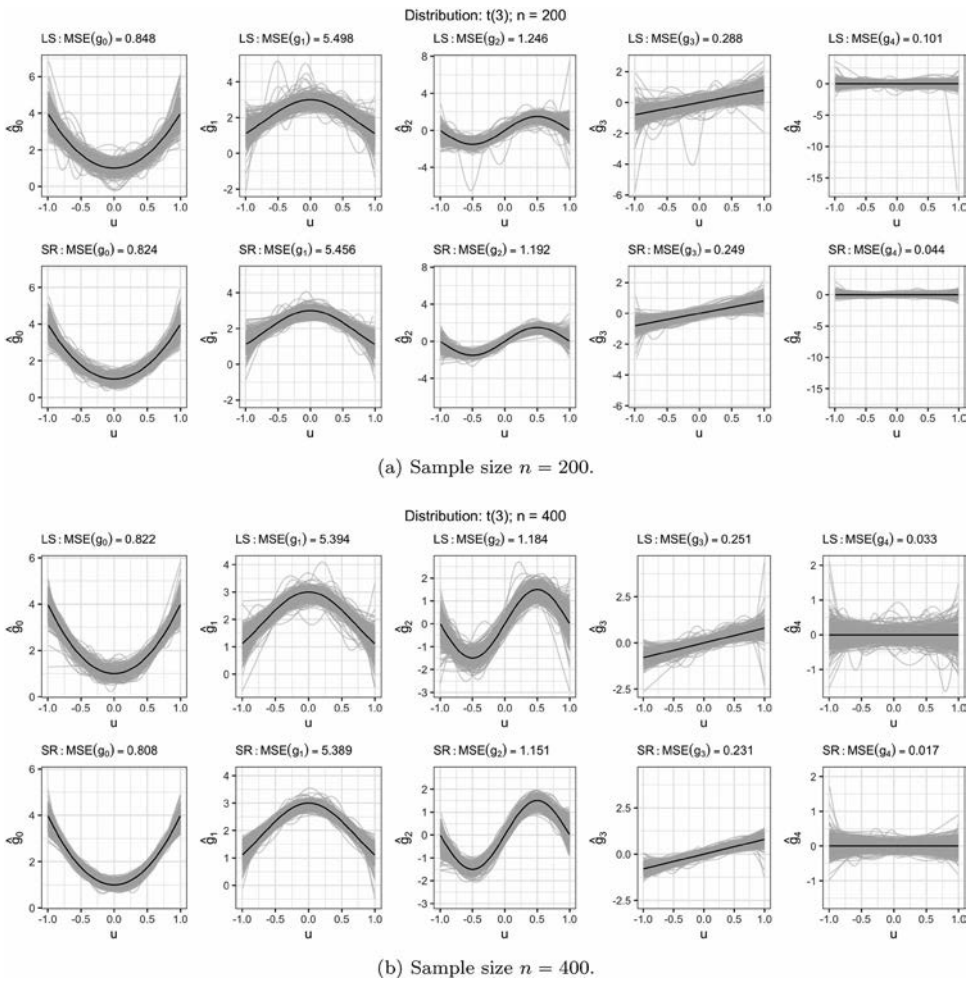

Figure 9. Individual smooths $\{g_0, g_1, g_2, g_3, g_4\}$ for a varying coefficient model with $t(3)$ errors estimated using penalized least squares (LS) and signed-rank (SR) methods for 500 simulations (in grey), with the true functions overlaid in black.

For the second model, we fit a VCM where SST is a predictor with a functional coefficient of space and time,

$$Y_{(u,v,t)} = z_1(u, v, t) + z_2(u, v, t) \cdot SST_{(u,v,t)} + \varepsilon_{(u,v,t)}\ , \tag{4}$$

where z_1 and z_2 are three-dimensional tensor smoothing functions; location is defined as in the spatio-temporal formulation; and t is time in years from 1987 to 2012 due to the five-year SST lag. Since five years of data were lost due to the lagged SST calculations, the sample size decreased to 2362 for sablefish and 1804 for Pacific cod using this model. The same distribution assumptions given previously were also employed for this model.

For each model and each species' response, we reported the proportion of deviance explained, a generalization of r^2, as a measure of model fit and prediction [54]. We also performed a 10-fold cross-validation to evaluate the model prediction accuracy. To estimate

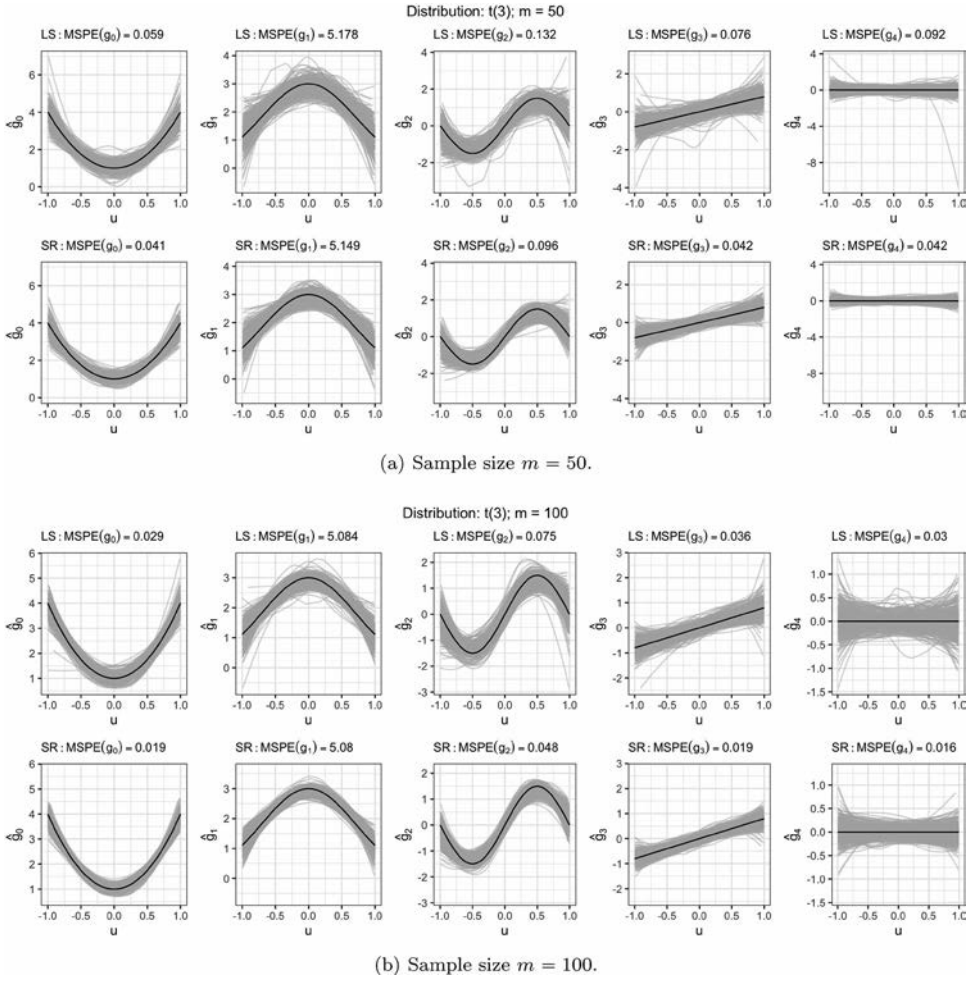

Figure 10. Individual smooths $\{g_0, g_1, g_2, g_3, g_4\}$ for a varying coefficient model with $t(3)$ errors predicted for a test data set of size m using penalized least squares (LS) and signed-rank (SR) methods for 500 simulations (in grey), with the true functions overlaid in black.

the cross-validation prediction error (CVE), we calculated the median absolute deviation for each fold and averaged across all folds. The proportion of variance explained and CVE from the two models fit for sablefish CPUE are given in Table 1. Table 2 shows the results for the two models fit on Pacific cod using the two distribution assumptions.

CVE was lower for the SR estimation method than the penalized LS method for all models (Tables 1 and 2). In the case of Pacific cod, SR gives higher variance explained and lower prediction error that further improve with the use of the bent score function. Proportion of variance explained values are higher for SR than LS-based VCM estimation across all models, showing SR estimation produces better fit and prediction. Including SST in the model increased the variance explained by the model as expected. It also lowered CVE for both sablefish and Pacific cod catch. Therefore, fisheries managers estimating sablefish

Table 1. Proportion of variance explained (Var. expl.) and cross-validation prediction error (CVE) for penalized least squares (LS) and signed-rank (SR) estimation procedures.

	Method	Var. expl.	CVE
Model 1	LS	0.776	0.981
	SR	0.848	0.912
Model 2	LS	0.828	0.861
	SR	0.903	0.769

Note: Varying coefficient models for sablefish CPUE: Model 1 is $Y_{(u,v,t)} = z_1(u,v,t) + \varepsilon_{(u,v,t)}$ and Model 2 is $Y_{(u,v,t)} = z_1(u,v,t) + z_2(u,v,t) \cdot SST_{(u,v,t)} + \varepsilon_{(u,v,t)}$.

Table 2. Proportion of variance explained (Var. expl.) and cross-validation prediction error (CVE) for penalized least squares (LS), signed-rank (SR), and signed-rank with bent score function (SR-bent) estimation procedures.

	Method	Var. expl.	CVE
Model 1	LS	0.841	0.170
	SR	0.909	0.156
	SR-bent	0.921	0.152
Model 2	LS	0.875	0.147
	SR	0.937	0.133
	SR-bent	0.945	0.130

Note: Varying coefficient models for Pacific cod CPUE: Model 1 is $Y_{(u,v,t)} = z_1(u,v,t) + \varepsilon_{(u,v,t)}$ and Model 2 is $Y_{(u,v,t)} = z_1(u,v,t) + z_2(u,v,t) \cdot SST_{(u,v,t)} + \varepsilon_{(u,v,t)}$.

or Pacific cod catch in the waters surrounding Alaska can achieve better predictions by including SST into their models.

5. Conclusion and discussion

The application of signed-rank-estimated VCMs to fisheries data produced increased deviance explained and decreased prediction error. This highlights the usefulness of the signed-rank method for prediction of ecological data where the VCM structure is appropriate. We have also illustrated that lower prediction error for skewed distributions using signed-rank estimation can be achieved by using appropriate bent score functions under a Gaussian distribution. Figure 11 shows the scaled residuals for Pacific cod catch using the VCM with a spatiotemporally variant SST fit with the classical penalized LS procedure and our proposed signed-rank procedure using the bent score function. Similar to the sablefish CPUE residuals presented already, the signed-rank approach was less influenced by outliers in Pacific cod CPUE than the classical VCM method. The use of VCMs for modeling spatial data in many areas of ecology is common [4,50,55], and the fisheries community has used these models extensively over the past two decades to track population and catch changes [45,46,49]. Typically, spatial covariates and time are considered additive with separate smoothing functions [11,34,36,48]. These types of models assume that the response trends over time have sufficiently similar patterns over all locations. For data that cover large areas, such as tracts of ocean typically observed in fisheries data, this

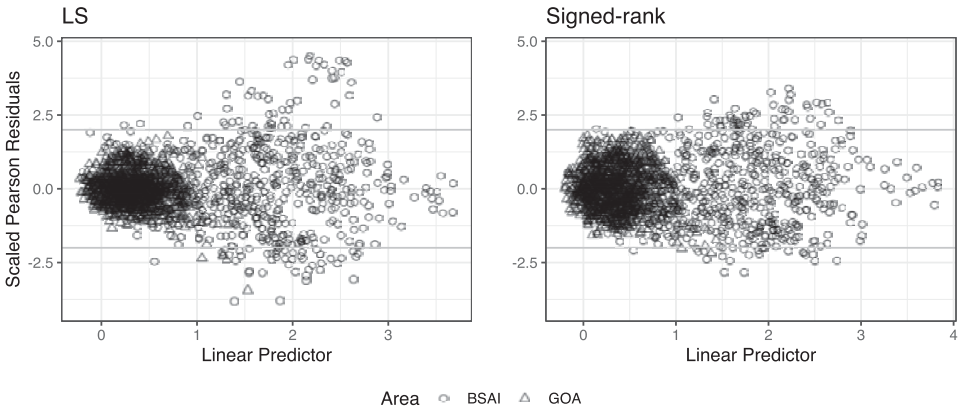

Figure 11. Scaled Pearson residuals plotted by area for Pacific cod CPUE modeled with a spatiotemporally variant sea surface temperature fit using penalized least squares (LS) or the signed-rank procedure with bent score function. BSAI = Bering Sea and Aleutian Islands; GOA = Gulf of Alaska.

assumption is unlikely to be supported. Given the highly variable nature of biological systems, a more suitable supposition is that the pattern of response over time is likely to vary based on the location. In fisheries studies, the spatiotemporal model is not commonly used to model catch or population size by considering the response to change over location and time simultaneously [3,5,51]. Using the three-dimensional tensor models allowed for estimating catch or population changes over time for each location point, thereby gaining a better understanding of whether locations share certain response patterns.

By illustration, we plotted each station's fitted sablefish and Pacific cod CPUE values against time in years using Equation (3) (Figure 12). The station-location effect in sablefish and Pacific cod catch may point to spatial differences in environment affecting fish catches in two distinct geographic regions. The stations occupying the Bering Sea, Aleutian

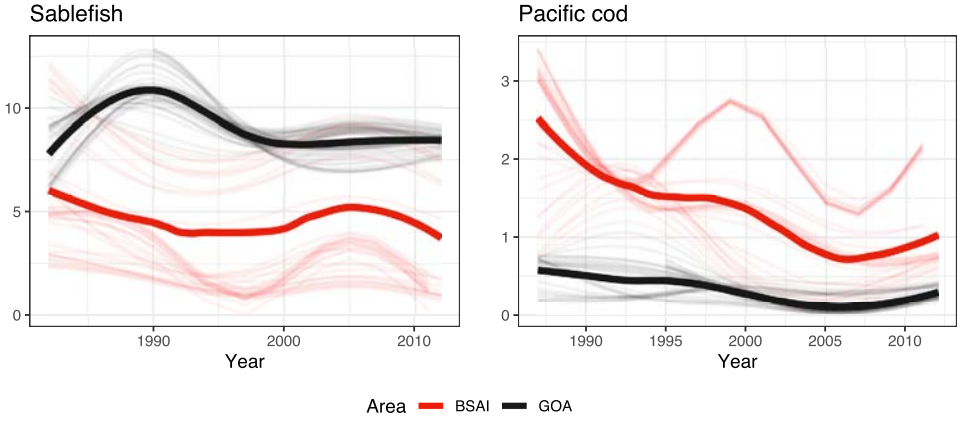

Figure 12. Sablefish (left) and Pacific cod (right) CPUE modeled by Equation 3 using 3D spatiotemporal smoothers.

Islands, and Western Gulf of Alaska management areas (BSAI) in the MESA longline survey [1] have a pattern of CPUE distinctive from stations in the Central Gulf, West Yakutat and East Yakutat/Southeast areas (GOA). Marked differences between the Gulf of Alaska area and the Bering Sea/Aleutian Islands region in ocean currents, sea-level pressure, and changes in mixed layer depths are known to exist [16]. Distinct variations in these factors have many potential pathways through which to transfer effects of climate to marine life. Large variations in the flow of the Alaskan Stream, an extension of the warm-water Alaskan Current which flows from Kodiak southwest along the Alaskan Peninsula, have been observed [40]. These variations do not persist near the Aleutians due to the stream rejoining its split inflow around 165°W. Identical marine taxa in nearby regions have been shown to display opposing responses within the same climate regime shift [8]. The split in catch trends of both sablefish and cod appears to support such evidence. Alaska's Unimak Pass, which approximately separates stations in the BSAI from those in the GOA, facilitates water transport from the Gulf of Alaska to the Bering Sea, and this fresher coastal water forms a front in the vicinity of the pass [41]. The distinction in catch trends is more apparent when observing stations closer to the Aleutian Islands and occupying the Bering Sea. The Bering Sea has colder water temperatures due to sea-ice melt and a cold subsurface pool in the summer, which creates a contrasting environment to the Gulf of Alaska region [8]. These differences are strongly tied to variations in primary production and are theorized to change trophic control in the Bering Sea ecosystem along with abundance of fishes, pinnipeds, and seabirds [24]. In turn, these ecosystem changes are expected to affect the wider North Pacific region in the future [18].

Heterogeneity over space and time should also be a consideration when including environmental and climatic variables in spatial and spatiotemporal VCMs, particularly for variables known to change over space and for datasets covering larger geographic regions. However, including spatially or spatiotemporally variant environmental factors has not been commonly adopted in ecological and fisheries management models [38]. The improvement in prediction for sablefish and Pacific cod CPUE when adding SST as a spatiotemporally varying environmental variable and evidence of temperature effects on early life histories in both fishes are strong indications that environmental conditions are important for accurate predictions and could contribute substantially to management decisions. While it is likely that SST has an impact on sablefish in the northeast Pacific, SST is not able to capture the full range of variability of regime shifts in the North Pacific. Regime shifts are also insufficient to explain climate variability in the region [31]. It is therefore necessary to consider other environmental and anthropogenic factors that may contribute to changes in catch rates in these complex marine systems. This would require models that include smoothing in higher dimensional spaces, perhaps taking advantage of sparsity in predictor matrices. Therefore, carefully considering and attempting to account for natural variability in biological systems using more dynamic and flexible models while maintaining predictive power through use of robust estimation methods can lead to more informative inferences and better predictions of changes in biological responses to environmental trends.

Disclosure statement

No potential conflict of interest was reported by the author(s).

Funding

This material is based upon work supported by the NSF Graduate Research Fellowship [grant 348 No. DGE-1414475] and NSF [grant number DMS-1343651].

ORCID

H. E. Correia http://orcid.org/0000-0003-3476-3674
A. Abebe http://orcid.org/0000-0001-5759-2383

References

[1] AFSC, *NOAA MESA: Longline Survey*, 2015. Available at http://www.afsc.noaa.gov/ABL/MESA/mesa_sfs_ls.php (accessed 14 April 2014).
[2] T. A'mar, J. Armstrong, K. Aydin, E. Conners, C. Conrath, M. Dalton, O. Davis, M. Dorn, K. Echave, C. Faunce, N. Friday, K. Green, D. Hanselman, J. Heifetz, P. Hulson, J. Ianelli, D. Jones, M. Jaenicke, A. Kingham, K.V. Kirk, S. Lowe, C. Lunsford, A. McCarthy, C. McGilliard, S. Meyer, R. Narita, D. Nichol, O. Ormseth, W. Palsson, C. Rodgveller, J. Rumble, K. Shotwell, L. Slater, K. Spalinger, P. Spencer, I. Spies, J. Stahl, I. Stewart, M. Stichert, W. Stockhausen, D. Stram, T. TenBrink, C. Tribuzio, J. Turnock, and T. Wilderbuer, *Stock assessment and fishery evaluation report for the groundfish resources of the Gulf of Alaska*, Tech. Rep., North Pacific Fishery Management Council, Anchorage, Alaska, (2015).
[3] S. Arcuti, C. Calculli, A. Pollice, G. D'Onghia, P. Maiorano, and A. Tursi, *Spatio-temporal modelling of zero-inflated deep-sea shrimp data by tweedie generalized additive*, Statistics 73 (2013), p. 87.
[4] N.H. Augustin, M. Musio, K. von Wilpert, E. Kublin, S.N. Wood, and M. Schumacher, *Modeling spatiotemporal forest health monitoring data*, J. Amer. Statist. Assoc. 104 (2009), pp. 899–911.
[5] N.H. Augustin, V.M. Trenkel, S.N. Wood, and P. Lorance, *Space-time modelling of blue ling for fisheries stock management*, Environmetrics 24 (2013), pp. 109–119.
[6] M. Austin, *Spatial prediction of species distribution: An interface between ecological theory and statistical modelling*, Ecol. Model. 157 (2002), pp. 101–118.
[7] K. Aydin, S. Barbeaux, D. Barnard, L. Chilton, B. Clark, M. Conners, C. Conrath, M. Dalton, K. Echave, L. Fritz, M. Furuness, D. Hanselman, A. Haynie, J. Hoff, T. Honkalehto, P. Hulson, J. Ianelli, S. Kotwicki, R. Lauth, S. Lowe, C. Lunsford, C. McGilliard, D. McKelvey, D. Nichol, B. Norcross, O. Ormseth, W. Palsson, C. Rodgveller, C. Rooper, P. Spencer, I. Spies, W. Stockhausen, D. Stram, T. TenBrink, G. Thompson, C. Tribuzio, T. Wilderbuer, and N. Williamson, *Stock assessment and fishery evaluation report for the groundfish resources of the Bering Sea/Aleutian Islands regions*, Tech. Rep., North Pacific Fishery Management Council, Anchorage, Alaska, (2015).
[8] A.J. Benson and A.W. Trites, *Ecological effects of regime shifts in the Bering Sea and eastern North Pacific Ocean*, Fish Fish. 3 (2002), pp. 95–113.
[9] B.A. Brumback and J.A. Rice, *Smoothing spline models for the analysis of nested and crossed samples of curves*, J. Amer. Statist. Assoc. 93 (1998), pp. 961–976.
[10] W.S. Cleveland, E. Grosse, W.M. Shyu, J.M. Chambers, and T.J. Hastie, *Statistical Models in S Local Regression Models*, Chapman & Hall/CRC, Boca Raton, 1992.
[11] v. Denis, J. Lejeune, and J.p. Robin. *Spatio-temporal analysis of commercial trawler data using general additive models: Patterns of loliginid squid abundance in the north-east atlantic*, ICES J. Mar. Sci. J. Du Con. 59 (2002), pp. 633–648.
[12] C.F. Dormann, *Effects of incorporating spatial autocorrelation into the analysis of species distribution data*, Glob. Ecol. Biogeogr. 16 (2007), pp. 129–138.
[13] K. Echave, C. Rodgveller, and S. Shotwell, *Calculation of the geographic area sizes used to create population indices for the Alaska Fisheries Science Center longline survey*, Tech. Rep. NMFS-AFSC-253, National Oceanic and Atmospheric Administration (NOAA), 2013. NOAA Technical Memorandum NMFS-AFSC-253
[14] J. Fan and I. Gijbels, *Local Polynomial Modelling and Its Applications: Monographs on Statistics and Applied Probability*, Vol. 66, CRC Press, Boca Raton, 1996.

[15] J.A.D. Fisher, M. Casini, K.T. Frank, C. Möllmann, W.C. Leggett, and G. Daskalov, *The importance of within-system spatial variation in drivers of marine ecosystem regime shifts*, Philos. Trans. Royal Soc. Lond. B Biol. Sci. 370 (2014). Available at http://rstb.royalsocietypublishing.org/content/370/1659/20130271.
[16] R.C. Francis, S.R. Hare, A.B. Hollowed, and W.S. Wooster, *Effects of interdecadal climate variability on the oceanic ecosystems of the NE pacific*, Fish. Oceanogr. 7 (1998), pp. 1–21. Available at http://dx.doi.org/10.1046/j.1365-2419.1998.00052.x.
[17] A.E. Gelfand, H.J. Kim, C. Sirmans, and S. Banerjee, *Spatial modeling with spatially varying coefficient processes*, J. Amer. Statist. Assoc. 98 (2003), pp. 387–396.
[18] J.M. Grebmeier, J.E. Overland, S.E. Moore, E.V. Farley, E.C. Carmack, L.W. Cooper, K.E. Frey, J.H. Helle, F.A. McLaughlin, and S.L. McNutt, *A major ecosystem shift in the northern Bering Sea*, Sci. 311 (2006), pp. 1461–1464.
[19] A. Guisan, T.C.E. Jr, and T. Hastie, *Generalized linear and generalized additive models in studies of species distributions: Setting the scene*, Ecol. Model. 157 (2002), pp. 89–100.
[20] N. Hamm, A. Finley, M. Schaap, and A. Stein, *A spatially varying coefficient model for mapping PM10 air quality at the european scale*, Atmos. Environ. 102 (2015), pp. 393–405.
[21] T.J. Hastie and R.J. Tibshirani, *Generalized Additive Models*, London, Chapman and Hall, Ltd., 1990 (Monographs on Statistics and Applied Probability; 43).
[22] T.P. Hettmansperger and J.W. McKean, *Robust Nonparametric Statistical Methods*, 2nd ed., Boca Raton, FL, CRC Press; 2011. (Monographs on Statistics and Applied Probability; 119).
[23] J.A. Hoeting, *The importance of accounting for spatial and temporal correlation in analyses of ecological data*, Ecol. Appl. 19 (2009), pp. 574–577. Available at http://dx.doi.org/10.1890/08-0836.1.
[24] G.L. Hunt Jr, P. Stabeno, G. Walters, E. Sinclair, R.D. Brodeur, J.M. Napp, and N.A. Bond, *Climate change and control of the southeastern Bering Sea pelagic ecosystem*, Deep Sea Res. Part II Topical Stud. Oceanogr. 49 (2002), pp. 5821–5853. Ecology of the {SE} Bering Sea.
[25] T.P. Hurst, S.B. Munch, and K.A. Lavelle, *Thermal reaction norms for growth vary among cohorts of pacific cod (Gadus macrocephalus)*, Mar. Biol. 159 (2012), pp. 2173–2183. Available at http://dx.doi.org/10.1007/s00227-012-2003-9.
[26] J. Kloke and J.W. McKean, *Nonparametric Statistical Methods Using R*, CRC Press, New York, 2014.
[27] B.J. Laurel, T.P. Hurst, L.A. Copeman, and M.W. Davis, *The role of temperature on the growth and survival of early and late hatching pacific cod larvae (Gadus macrocephalus)*, J. Plankton Res. 30 (2008), pp. 1051–1060.
[28] B.J. Laurel, M. Spencer, P. Iseri, and L.A. Copeman, *Temperature-dependent growth and behavior of juvenile Arctic cod (Boreogadus saida) and co-occurring north pacific gadids*, Polar Biol. 39 (2016), pp. 1127–1135.
[29] P. Legendre and M.J. Fortin, *Spatial pattern and ecological analysis*, Veg. 80 (1989), pp. 107–138. Available at http://dx.doi.org/10.1007/BF00048036.
[30] A.M. Liebhold and J. Gurevitch, *Integrating the statistical analysis of spatial data in ecology*, Ecography 25 (2002), pp. 553–557.
[31] M.A. Litzow, F.J. Mueter, and A.J. Hobday, *Reassessing regime shifts in the north pacific: Incremental climate change and commercial fishing are necessary for explaining decadal-scale biological variability*, Glob. Change Biol. 20 (2014), pp. 38–50.
[32] Z. Lu, D.J. Steinskog, D. Tjøstheim, and Q. Yao, *Adaptively varying-coefficient spatiotemporal models*, J. R. Stat. Soc. Ser. B (Stat. Methodol.) 71 (2009), pp. 859–880.
[33] G.V.M. Miakonkana and A. Abebe, *Iterative rank estimation for generalized linear models*, J. Statist. Plann. Inference 151/152 (2014), pp. 60–72. MR 3216638
[34] B.L. Mourato, F. Hazin, K. Bigelow, M. Musyl, F. Carvalho, and H. Hazin, *Spatio-temporal trends of sailfish istiophorus platypterus catch rates in relation to spawning ground and environmental factors in the equatorial and Southwestern Atlantic Ocean*, Fish. Oceanogr. 23 (2014), pp. 32–44.
[35] NOAA, *National Data Buoy Center – Optimum Interpolation Sea Surface Temperature*, 2015. Available at https://www.ncdc.noaa.gov/oisst (accessed 18 September 2015).
[36] S. Ortega-García, E. Camacho-Bareño, and R.O. Martínez-Rincón, *Effects of environmental factors on the spatio-temporal distribution of striped marlin catch rates off Cabo San Lucas, Baja*

California Sur, Mexico, Fish. Res. 166 (2015), pp. 47–58. Proceedings of the 5th International Billfish Symposium.
[37] S. Pennoyer and J. Balsiger, *Groundfish total allowable catch specifications and prohibited species catch limits under the authority of the fishery management plans for the groundfish fishery of the Bering Sea and Aleutian Islands area and groundfish of the Gulf of Alaska: Final supplemental environmental impact statement*, Tech. Rep., United States National Marine Fisheries Service Alaska Regional Office, Juneau, Alaska, 1998.
[38] A.J. Phillips, L. Ciannelli, R.D. Brodeur, W.G. Pearcy, and J. Childers, *Spatio-temporal associations of Albacore CPUEs in the Northeastern Pacific with regional SST and climate environmental variables*, ICES J. Mar. Sci. J. Du Cons. 71 (2014), pp. 1717–1727.
[39] R Core Team. *R: A Language and Environment for Statistical Computing*, R Foundation for Statistical Computin, Vienna, Austria, 2020. Available at https://www.R-project.org/.
[40] R. Reed, *Flow of the Alaskan stream and its variations*, Deep Sea Res. A 31 (1984), pp. 369–386.
[41] J.D. Schumacher, C.A. Pearson, and J.E. Overland, *On exchange of water between the Gulf of Alaska and the Bering Sea through unimak pass*, J Geophys. Res. Oceans (1978–2012) 87 (1982), pp. 5785–5795.
[42] G.L. Sievers and A. Abebe, *Rank estimation of regression coefficients using iterated reweighted least squares*, J. Stat. Comput. Simul. 74 (2004), pp. 821–831. MR 2083105
[43] S.M. Sogard and B.L. Olla, *Contrasting behavioral responses to cold temperatures by two marine fish species during their pelagic juvenile interval*, Environ. Biol. Fishes 53 (1998), pp. 405–412.
[44] S.M. Sogard and B.L. Olla, *Growth and behavioral responses to elevated temperatures by juvenile sablefish Anoplopoma fimbria and the interactive role of food availability*, Mar. Ecol. Prog. Ser. 217 (2001), pp. 121–134.
[45] D. Sohn, L. Ciannelli, and J. Duffy-Anderson, *Distribution of early life pacific halibut and comparison with Greenland halibut in the eastern Bering Sea*, J. Sea Res. 107 (2016), pp. 31–42. Proceedings of the Ninth International Symposium on Flatfish Ecology.
[46] P. Sousa, M. Azevedo, and M.C. Gomes, *Species-richness patterns in space, depth, and time (1989–1999) of the Portuguese fauna sampled by bottom trawl*, Aquat. Living Resour. 19 (2006), pp. 93–103.
[47] L.C. Stige, P. Dalpadado, E. Orlova, A.C. Boulay, J.M. Durant, G. Ottersen, and N.C. Stenseth, *Spatiotemporal statistical analyses reveal predator-driven zooplankton fluctuations in the barents sea*, Prog. Oceanogr. 120 (2014), pp. 243–253.
[48] N.J. Su, C.L. Sun, A.E. Punt, and S.Z. Yeh, *Environmental and spatial effects on the distribution of blue marlin (Makaira nigricans) as inferred from data for longline fisheries in the Pacific Ocean*, Fish. Oceanogr. 17 (2008), pp. 432–445.
[49] G. Swartzman, C. Huang, and S. Kaluzny, *Spatial analysis of Bering Sea groundfish survey data using generalized additive models*, Can. J. Fish. Aquat. Sci. 49 (1992), pp. 1366–1378.
[50] M. Torabi, *Spatiotemporal modeling of odds of disease*, Environmetrics 25 (2014), pp. 341–350.
[51] B.L. Townhill, D. Maxwell, G.H. Engelhard, S.D. Simpson, and J.K. Pinnegar, *Historical Arctic logbooks provide insights into past diets and climatic responses of cod*, PLoS. ONE. 10 (2015), pp. 1–15.
[52] P. Whittle, *On stationary processes in the plane*, Biometrika 41 (1954), pp. 434–449.
[53] S.N. Wood, *Generalized Additive Models: An Introduction with R*, 2nd ed., Chapman and Hall/CR, 2017.
[54] S.N. Wood, *Generalized Additive Models*, Chapman and Hall/CRC, Boca Raton, FL, 2006 (Texts in Statistical Science Series).
[55] D.G. Woolford, D.R. Bellhouse, W.J. Braun, C.B. Dean, D.L. Martell, and J. Sun, *A spatio-temporal model for people-caused forest fire occurrence in the Romeo Malette forest*, J. Environ. Stat. 2 (2011), pp. 2–26.
[56] H. Zhu, J. Fan, and L. Kong, *Spatially varying coefficient model for neuroimaging data with jump discontinuities*, J. Amer. Statist. Assoc. 109 (2014), pp. 1084–1098.